

Solid-State Circuit for Spin Entanglement Generation and Purification

J. M. Taylor,¹ W. Dür,^{2,3} P. Zoller,^{2,3} A. Yacoby,^{1,4} C. M. Marcus,¹ and M. D. Lukin¹

¹Department of Physics, Harvard University, Cambridge, Massachusetts 02138, USA

²Institut für Theoretische Physik, Universität Innsbruck, Technikerstraße 25, A-6020 Innsbruck, Austria

³Institut für Quantenoptik und Quanteninformation der Österreichischen Akademie der Wissenschaften, Innsbruck, Austria

⁴Department of Condensed Matter Physics, Weizmann Institute of Science, Rehovot 76100, Israel

(Received 10 March 2005; published 15 June 2005)

We show how realistic charge manipulation and measurement techniques, combined with the exchange interaction, allow for the robust generation and purification of four-particle spin entangled states in electrically controlled semiconductor quantum dots. The generated states are immunized to the dominant sources of noise via a dynamical decoherence-free subspace; all additional errors are corrected by a purification protocol. This approach may find application in quantum computation, communication, and metrology.

DOI: 10.1103/PhysRevLett.94.236803

PACS numbers: 73.63.Kv, 03.67.Mn, 03.67.Pp

Entangled states are a basic resource for quantum information processing, including quantum communication, teleportation, measurement-based quantum computation [1], and quantum-based metrology. Einstein-Podolsky-Rosen (EPR) pairs exemplify entangled states, contributing both to theoretical insight into the nature of entanglement and to experimental proofs of Bell's inequalities [2]. In addition, entangled pairs are a fundamental component in scaling up quantum computers by connecting small-scale processors in a quantum network. EPR pair generation and purification is traditionally discussed in the context of long distance quantum communication via photons in a quantum repeater setup. In the presence of errors in noisy communication channels, robust generation of high-fidelity EPR pairs can be achieved via purification [3–5], where a single high-quality pair is distilled in a probabilistic manner from many low-fidelity singlets. In a solid-state environment, these ideas remain relevant, for example, for spin-based qubits in quantum dots, from the perspective of connecting “distant” parts of mesoscopic circuits, as well as from the more fundamental perspective of protection of entanglement in a complex environment. This Letter develops a protocol for generation and purification of electron spin-based EPR pairs in mesoscopic circuits, which builds directly on emerging experimental techniques, and is tailored to the specific decoherence mechanisms in a semiconductor environment.

We consider a setup consisting of an array of electrically gated quantum dots (see Fig. 1), where electrons, with spin representing the qubit, can be transported by applying appropriate gate voltages [[6,7], Fig. 1(b)]. In its simplest form, a nonlocal EPR pair of electrons can be produced by local preparation of a ground singlet state of two electrons in one of the quantum dots, splitting the pair into two adjacent dots and shuttling the electrons to the end nodes. A *purification protocol* corrects for qubit errors from transport and storage. Our strategy is to develop such a purification protocol on a more advanced level, where the qubits are encoded in *logical states* of a decoherence-free sub-

space (DFS) of two electrons, which from the beginning immunizes our logical qubits against the dominant source of decoherence, represented by hyperfine interactions. Thus the goal is to produce local pairs of *logical entangled states*, represented by four entangled electrons, transport logical pairs to the end nodes, and run an Oxford-type [4] purification protocol on these logical qubits that corrects all errors. We will show below that exchange interactions and (partial) Bell measurements for the physical qubits are sufficient to implement this protocol. We remark that the required physical resources are already available at present in the lab.

Choice of encoded states.—We begin by describing a specific encoding that allows suppression of the dominant error mechanism. We focus on hyperfine effects as theory and experiment have demonstrated their detrimental effect on electron spin coherences (dephasing), with $T_2^* \sim 10$ ns [8,9], while spin-orbit-phonon and other spin-flip processes (relaxation) are observed to enter only for times on the order of 1 ms in the presence of a large magnetic

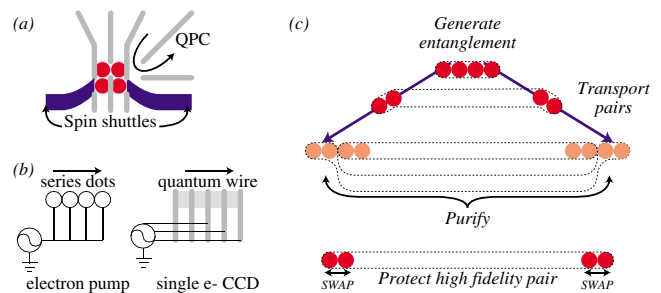


FIG. 1 (color online). (a) Schematic outline of a node, as it might be implemented in a gate-defined quantum dot (red). A nearby quantum point contact (QPC) measures charge, gates (gray) are pulsed for state generation and control, and spin transport channels (blue) allow the entangled state to be sent to distant locations. (b) Schematic outline of two spin transport channels: electron pump and single electron CCD. (c) Overview of robust entanglement generation.

field [10,11]. Given the long correlation time of the electron spin-nuclear spin interaction [12,13], storing entanglement in the logical states of a DFS with total S_z quantum number $m_s = 0$, $|0_L\rangle = (|\uparrow\downarrow\rangle - |\downarrow\uparrow\rangle)/\sqrt{2}$, and $|1_L\rangle = (|\uparrow\uparrow\rangle + |\downarrow\downarrow\rangle)/\sqrt{2}$, allows for suppression of such dephasing by repeatedly exchanging the two electrons [14]. The four-particle entangled state

$$|\phi^+\rangle = |0_L\rangle|0_L\rangle + |1_L\rangle|1_L\rangle = |\uparrow\uparrow\downarrow\downarrow\rangle + |\downarrow\downarrow\uparrow\uparrow\rangle \quad (1)$$

takes full advantage of these properties, suppressing phase noise. This combination of subspace choice and exchanging electrons corresponds to a dynamical DFS (DDFS) and is a de facto implementation of Carr-Purcell spin echo in the DFS. We show below that using a DDFS, memory and transport errors will be dominated by spin-flip terms, an improvement of order 10^5 over hyperfine-related noise. Errors in the DDFS procedure, and spin-flip errors, are so far uncorrected. Starting with several copies of the entangled state $|\phi^+\rangle$, our purification protocol corrects for spin-flip errors entirely, by detection of the total m_s quantum number of the states, while it corrects for phase errors by analogy to the protocol of Ref. [4].

We now consider the ingredients and recipe for EPR pair generation and purification in the DDFS: (I) charge manipulation and measurement techniques for performing exchange gates ($U_{AB}(\phi)$), singlet generation, and partial Bell state measurements M_{AB} ; (II) the dynamical DFS's properties with regards to different noise sources, its behavior during storage (memory) and transport, to show suppression of better than 10^5 for low frequency phase noise; (III) a purification protocol that works in the encoded space and corrects for arbitrary errors, using only the partial Bell state measurement and exchange gate described in (I).

(I). *Charge manipulation and measurement.*—We suggest an implementation of the necessary resources for each node: exchange gate, singlet generation, and partial 2 electron Bell state measurement. In principle, other techniques could be used to generate the same set of operations.

The Loss-Divincenzo exchange gate [15] between two electrons in separate dots, A and B , is defined as $U_{AB}(\phi) = \exp(-i\phi\vec{S}^A \cdot \vec{S}^B)$; for example, $U(\pi/8)$ is $\sqrt{\text{SWAP}}$. By control of the tunnel coupling T_c between A and B , or by changing their relative bias, arbitrary ϕ may be achieved. It requires only pulsed-gate manipulation; i.e., it relies on charge control.

Singlet states of double dots may be created using the large exchange splitting of single dots. For a double-dot system, starting in the $(1, 0)$ stability island [Fig. 2(a)] resets the state of the double-dot (position A); changing configuration to the $(2, 0)$ stability island (position B) and coupling to the leads results in a singlet state of $(2, 0)$ ($|S_{(2,0)}\rangle$) if the single dot exchange is large, $J_{(2,0)} \gg k_b T$, which prevents filling of the triplet states. We remark that this is the only strict temperature requirement in this Letter. Adiabatically changing the bias of the double-dot system

to the $(1, 1)$ stability island [position C, Fig. 2(b)] results in adiabatic passage of the $(2, 0)$ singlet to the $(1, 1)$ singlet ($|S_{(1,1)}\rangle = (|\uparrow\downarrow\rangle - |\downarrow\uparrow\rangle)_{(1,1)}/\sqrt{2}$). If this is accomplished much faster than dephasing mechanisms, the $(1, 1)$ singlet can be prepared with high fidelity. Assuming a linear ramp of detuning with a time τ , the probability of error goes as $\pi(\tau/T_2^*)^2[10^{-2} + (\hbar/\epsilon_z T_2^*)^2]$; for $\tau = 1$ ns and $T_2^* = 10$ ns, the fidelity is >0.99 .

In addition, we can exploit the double-dot system to make a partial Bell measurement that leaves the logical subspace of our system untouched (up to a correctable phase). To achieve this, two spins are placed separated but adjacent quantum dots and the detuning is adiabatically changed from position C to position B. Only the singlet ($|S\rangle$) transfers; waiting a time t_1 in this configuration allows a charge measurement to distinguish between $(2, 0)$ ($|S\rangle$ result) and $(1, 1)$ (one of three triplet states). Adiabatically returning to C and waiting a time T_2^* switches the singlet and $m_s = 0$ triplet ($|T_0\rangle$) states with probability $1/2$. Going again to B, if the triplet state was switched to $|S\rangle$, it transfers to $(2, 0)$, producing a noticeable charge signal. Repeating this process k times can generate, with probability $1 - 1/2\sqrt{k}$, a charge signal for the $m_s = 0$ subspace; the total time for charge measurement is $t_M/2 \approx k(T_2^* + t_m) + t_1$, where t_m is the time to make a single

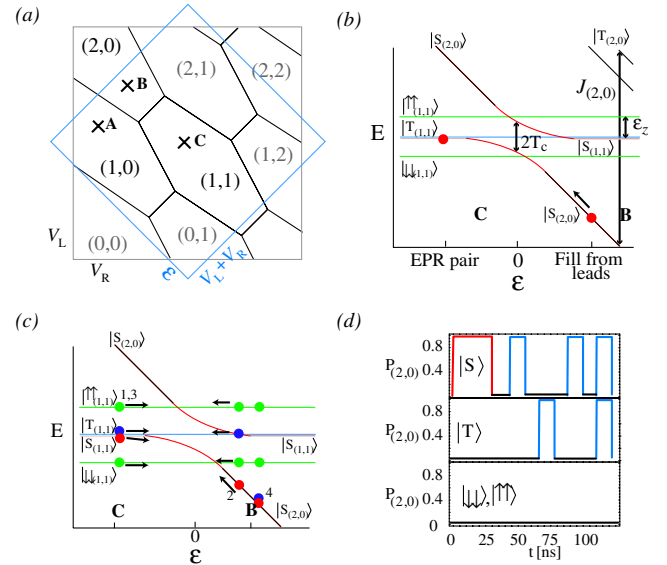


FIG. 2 (color online). (a) Stability diagram of a double-dot system, with gate voltages for left and right dots, V_L, V_R , and alternative axes of detuning and total voltage, $\epsilon, V_L + V_R$. The three positions A, B, and C are marked. (b) Energy level diagram for detuning between B and C. An external magnetic field Zeeman (ϵ_z) splits the triplet levels of the $(1, 1)$ configuration; tunnel coupling leads to an avoided crossing at $\epsilon = 0$; by starting in $|S_{(2,0)}\rangle$ at B and adiabatically changing ϵ to C, a separated singlet is generated. (c) The four stage measurement procedure, as described in the text. (d) Example signals of the measurement for four possible initial states, as labeled; section in red occurs only for $|S\rangle$; blue only for $|S\rangle, |T_0\rangle$.

charge measurement. In our present implementation, long t_m may be the main limitation for the purification protocol discussed below [16]. The three results of measurement are (a) singlet, (b) $m_s = 0$ triplet, or (c) $|m_s| = 1$. During this time, the $|m_s| = 1$ states remain untouched except for a phase; we now show how this measurement procedure, denoted M_{AB} , can generate our desired entangled state, $|\phi^+\rangle$, and adjust the phase for such a state.

Starting with four dots (1–4) [Fig. 1(c)], we prepare singlets in 12 and 34; this initial state is $|S\rangle_{12}|S\rangle_{34}$. Applying M_{23} and keeping only the $|m_s| = 1$ result (occurring with probability 1/2) yields the state $|\phi^+\rangle$. To correct the accumulated phase error on it, we use a sequence: [wait($t_M/4$), SWAP₁₂, SWAP₃₄, M_{23} , SWAP₁₂, SWAP₃₄, wait($t_M/4$)], which we now study.

(II). *Dynamical DFS*.—We examine the dynamical DFS in detail with a general noise formulation. While we focus on hyperfine terms, other low frequency noise will be similarly corrected. To be specific, we assume a phase noise term $\eta(t)$ acts on electron spins, characterized by a power spectrum, $S(\omega)$, of integrated power $(T_2^*)^2$ with a (possibly polynomial) high frequency cutoff at $\gamma \ll 1/T_2^*$. For example, the hyperfine interaction in quantum dots, with long-time scale non-Markovian dynamics, is well described by this process [13].

In a frame rotating with external magnetic field (which also defines up and down spin), the phase term acts on a spin state as $|\uparrow\rangle \pm |\downarrow\rangle \rightarrow |\uparrow\rangle \pm e^{-i \int_0^t \eta(t') dt'} |\downarrow\rangle$. Using two electron spins in separate, adjacent dots to create the encoded space, $|0_L\rangle, |1_L\rangle$, this action may be represented by a stochastic evolution operator, $U(t, 0) = e^{-i \int_0^t \eta(t') dt' \sigma_x^L}$, where σ_x^L is a Pauli matrix for the encoded space, i.e., flips the logical bit. As the dots are adjacent, they may easily be SWAPed. The pulse sequence [wait($\tau/4$), SWAP, wait($\tau/2$), SWAP, wait($\tau/4$)] gives a reduced power spectrum,

$$S_{\text{DDFS}}(\omega) = S(\omega) \frac{256}{\tau^2 \omega^2} \cos^2\left(\frac{\tau\omega}{8}\right) \sin^6\left(\frac{\tau\omega}{8}\right). \quad (2)$$

For frequencies below $1/\tau$, $S_{\text{DDFS}}(\omega) \simeq S(\omega) \frac{\tau^4 \omega^4}{1024}$; if the dominant noise mechanism has only low frequency components (such as hyperfine terms) the suppression can be dramatic. For SWAP operations performed by use of exchange gates, the gate must be performed in a time $\tau_{\text{ex}} \ll T_2^*$; with physical exchange of electrons, e.g., by use of an auxiliary dot, this requirement is relaxed.

The DFS also reduces phase errors incurred during transport of the electron spins. For example, two electrons forming a logical state are moved sequentially through the same channel (i.e., same series of quantum dots) with a separation time $\tau_T (\approx 4\sigma/v$, where σ is the lateral radius of each dot, and v the average velocity of transport). Replacing $\eta(t)$ with $\eta(x, t)$, we set $\langle \eta(x, t) \eta(x', t') \rangle = C(|x - x'|) \int_{-\infty}^{\infty} S(\omega) e^{i\omega(t-t')} d\omega$ for transport through a series of quantum dots, where $C(x) = e^{-x^2/2\sigma^2}$. The result-

ing spectral function is

$$S_T(\omega) = \int_{-\infty}^{\infty} S(\nu) \sin^2\left[\frac{\nu\tau_T}{2}\right] \frac{e^{-(\tau_T/4)^2(\nu-\omega)^2/2}}{\sqrt{2\pi(4/\tau_T)^2}} d\nu.$$

This shows a suppression of noise with frequencies $\ll 1/\tau_T$ by $\tau_T^2 \omega^2/8$.

Considering practical parameters, we set $\gamma = \gamma_{dd} = 1 \text{ ms}^{-1}$, $T_2^* = 10 \text{ ns}$, and use $S(\omega) = e^{-(\omega^2/2\gamma^2)}/(T_2^* \sqrt{2\pi\gamma^2})$. For states stored in the DDFS with a cycle time τ , after one cycle the probability of error is $p_{\text{err}} = \frac{3}{2^{12}} \frac{\gamma^4 \tau^6}{(T_2^*)^2}$. Transporting through $n = L/v$ quantum dots, we find the probability of a phase error occurring for the encoded states is $p_{\text{err},T}(n) \approx \sqrt{\frac{\pi}{128}} \left(\frac{\gamma}{T_2^*}\right)^2 \tau^4 n$. Even for cycle and transport times (τ, τ_T) approaching T_2^* , phase errors due to low frequency terms occur with rates much slower than milliseconds, indicating a suppression of more than 10^5 . Thus the dynamical DFS technique provides a powerful quantum memory and low-error transport channel, limited by errors in SWAP operations and spin-flip processes.

(III). *Purification*.—We now introduce a purification protocol for encoded entangled states that can remove all remaining errors, based on partial Bell measurement and exchange gates. Errors during the generation, transport, and storage processes can lead to (i) errors within the $\{|0_L\rangle, |1_L\rangle\}$ logical subspace and (ii) population of states $|2_L\rangle = 1/\sqrt{2}(|\uparrow\uparrow\rangle + |\downarrow\downarrow\rangle)$, $|3_L\rangle = 1/\sqrt{2}(|\uparrow\uparrow\rangle - |\downarrow\downarrow\rangle)$ outside the logical subspace. Both kinds of errors reduce the fidelity of the encoded entangled state $|\phi^+\rangle_{A_1 A_2 B_1 B_2}$ and need to be corrected. We introduce a purification protocol that completely corrects arbitrary strength errors of type (ii), and corrects for errors of type (i) that occur with probability less than 1/2.

We start by reviewing the measurement scheme [Fig. 2(c) and 2(d)], which has three possible outcomes: (a) P_S : measure $|S\rangle$, state after measurement is $|S\rangle$; (b) P_{T_0} : measure $|T_0\rangle = 1/\sqrt{2}(|\uparrow\uparrow\rangle + |\downarrow\downarrow\rangle)$, state is $|S\rangle$; (c) $P_{|m_s|=1}$: state is coherently projected into the two-dimensional subspace spanned by $\{|\uparrow\uparrow\rangle, |\downarrow\downarrow\rangle\}$. Consider the following sequence of measurements of this type with indicated results: $O_A^{(0)} = P_S^{(A'_1 A'_2)} P_{|m_s|=1}^{(A_1 A'_1)} P_{|m_s|=1}^{(A_2 A'_2)}$, $O_A^{(1)} = P_{T_0}^{(A'_1 A'_2)} P_{|m_s|=1}^{(A_1 A'_1)} P_{|m_s|=1}^{(A_2 A'_2)}$. The action of $O_A^{(k)}$ on logical basis states is given by

$$O_A^{(k)} |i_L\rangle_{A_1 A_2} |j_L\rangle_{A'_1 A'_2} = P_{\{0,1\}} |i_L \oplus j_L \oplus k\rangle_{A_1 A_2} |0_L\rangle_{A'_1 A'_2},$$

where the projector $P_{\{0,1\}}$ indicates that, in both A, A' , all components outside the $\{|0_L\rangle, |1_L\rangle\}$ subspace are projected out. The measurement sequence can thus be used to detect all errors of type (ii), while the operations $O_A^{(k)}$ act within the logical subspace similarly to a CNOT operation (\oplus denotes bitwise addition modulo 2).

Consider a mixed state $\rho_{A_1 A_2 B_1 B_2}$ resulting from imperfect distribution of $|\phi^+\rangle$. We decompose ρ into three

terms, $\rho = \rho(\vec{x}) + \rho_{\text{od}} + \rho_R$. We have $\rho(\vec{x}) = x_0|\phi^+\rangle \times \langle\phi^+| + x_1|\phi^-\rangle \langle\phi^-| + x_2|\psi^+\rangle \langle\psi^+| + x_3|\psi^-\rangle \langle\psi^-|$, where $|\phi^\pm\rangle = (|0_L 0_L\rangle \pm |1_L 1_L\rangle)/\sqrt{2}$ and $|\psi^\pm\rangle = (|0_L 1_L\rangle \pm |1_L 0_L\rangle)/\sqrt{2}$ are the logical Bell states. All off-diagonal elements in the Bell basis (ρ_{od}) and terms containing $\{|2_L\rangle, |3_L\rangle\}$ (ρ_R) are made irrelevant by the protocol.

Given two mixed states $\rho_{A_1 A_2 B_1 B_2} \otimes \rho'_{A'_1 A'_2 B'_1 B'_2}$, described by \vec{x} and \vec{x}' (and the irrelevant $\rho_{\text{od}} + \rho_R$), respectively, the following sequence of *local* operations obtains with certain probability a state with higher fidelity and hence purifies the state: (i) partial depolarization of ρ using, with probability $p = 1/2$, $\text{SWAP}_{A_1 A_2} \otimes \text{SWAP}_{B_1 B_2}$ or identity, and similarly for ρ' ; (ii) exchange gates $U(\pi/8)_{A_1 A_2} \otimes U(-\pi/8)_{B_1 B_2}$ at $\rho_{A_1 A_2 B_1 B_2}$ (and same for ρ'); (iii) sequence of measurements $O_A^{(k)}$, $O_B^{(l)}$; keep state $\rho_{A_1 A_2 B_1 B_2}$ only if $k = l$; i.e., the results in final measurement coincide in A and B .

The effect of (i) is to erase off-diagonal terms of the form $|\phi^\pm\rangle \langle\psi^\pm|$ which may contribute to the protocol. The operation in (ii) exchanges logical states $|\psi^+\rangle \leftrightarrow |\psi^-\rangle$ while keeping $|\phi^\pm\rangle$ invariant. Finally (iii) realizes—in addition to the projection into the $\{|0_L\rangle, |1_L\rangle\}$ logical subspace in A and B , which erases all terms ρ_R, ρ'_R —a purification map. In particular, we find that the remaining off-diagonal elements do not contribute and the action of the protocol can be described by the nonlinear mapping of corresponding vectors \vec{x}, \vec{x}' . The resulting state is of the form $\rho(\vec{y}) + \tilde{\rho}_{\text{od}}$ (note that $\rho_R = 0$), where

$$\begin{aligned} y_0 &= (x_0 x'_0 + x_2 x'_2)/N, & y_1 &= (x_1 x'_1 + x_3 x'_3)/N, \\ y_2 &= (x_1 x'_3 + x_3 x'_1)/N, & y_3 &= (x_0 x'_2 + x_2 x'_0)/N, \end{aligned} \quad (3)$$

and $N = x_0 x'_0 + x_2 x'_2 + x_1 x'_1 + x_3 x'_3 + x_1 x'_3 + x_3 x'_1 + x_0 x'_2 + x_2 x'_0$ is the probability of success of the protocol. This map is equivalent (up to a reduced success probability by a factor of 1/8) to the purification map obtained in Ref. [4] for nonencoded Bell states. It follows that iteration of the map—which corresponds to iteratively applying the purification procedure (i)–(iii) to two identical copies of states resulting from successful previous purification rounds—leads to a (encoded) maximally entangled state $|\phi^+\rangle$. That is, the map has $\vec{y} = (1, 0, 0, 0)$ as attracting fixed point whenever $x_0 > x_1 + x_2 + x_3$. We emphasize that *all* errors leading outside the logical subspace (in particular, all spin-flip errors), independent of their probability of occurrence, can be corrected. This implies that even states with a very small fidelity F can be purified, provided that errors within the logical subspace do not exceed probability 1/2.

Additionally, since the resulting maps are identical to those of [4], the purification protocol shows a similar robustness against noise in local control operations. That is, errors of the order of several percent in local control operations can be tolerated while still leading to purification. We also remark that methods such as (nested) entan-

glement pumping can be applied [17], which significantly reduces the required number of nodes.

While we have focused on gate controlled quantum dots, these ideas may find implementation in electro-optically manipulated small arrays of self-assembled quantum dots [18]. In general, the prescription for entanglement generation in solid-state environments we describe here could also be followed in other solid-state systems such as superconductor-based qubit designs [19]. We anticipate that such long-range entangled state generation will have wide application, in scalable quantum computer architectures and in tomography based on entangled states.

We gratefully acknowledge helpful conversations with J. Petta and A. Johnson. The work at Harvard was supported by ARO, NSF, Alfred P. Sloan Foundation, and David and Lucile Packard Foundation. The work at Innsbruck was supported by the ÖAW through project APART (W. D.), the European Union, Austrian Science Foundation, and the DFG.

-
- [1] D. Gottesman and I. L. Chuang, *Nature (London)* **402**, 390 (1999).
 - [2] A. Aspect, J. Dalibard, and G. Roger, *Phys. Rev. Lett.* **49**, 1804 (1982).
 - [3] C. H. Bennett *et al.*, *Phys. Rev. Lett.* **76**, 722 (1996).
 - [4] D. Deutsch *et al.*, *Phys. Rev. Lett.* **77**, 2818 (1996).
 - [5] H.-J. Briegel, W. Dür, J. I. Cirac, and P. Zoller, *Phys. Rev. Lett.* **81**, 5932 (1998).
 - [6] Y. Ono *et al.*, *J. Appl. Phys.* **97**, 031101 (2005).
 - [7] Moving the carriers of quantum information by charge manipulation is in direct analogy to ion traps: D. Kielpinski, C. Monroe, and D. Wineland, *Nature (London)* **417**, 709 (2002).
 - [8] A. S. Bracker *et al.*, *Phys. Rev. Lett.* **94**, 047402 (2005).
 - [9] A. C. Johnson *et al.*, cond-mat/0503687; J. Petta *et al.* (to be published).
 - [10] R. Hanson *et al.*, *Phys. Rev. Lett.* **91**, 196802 (2003).
 - [11] V. N. Golovach, A. Khaetskii, and D. Loss, *Phys. Rev. Lett.* **93**, 016601 (2004).
 - [12] M. Mehring, *High Resolution NMR Spectroscopy in Solids* (Springer-Verlag, Berlin, 1976).
 - [13] I. A. Merkulov, A. L. Efros, and M. Rosen, *Phys. Rev. B* **65**, 205309 (2002).
 - [14] L. A. Wu and D. A. Lidar, *Phys. Rev. Lett.* **88**, 207902 (2002).
 - [15] D. Loss and D. P. DiVincenzo, *Phys. Rev. A* **57**, 120 (1998).
 - [16] Alternatively, an external magnetic field gradient or slow adiabatic passage allows for deterministic rotation of $|T_0\rangle$ to $|S\rangle$ and greatly improves the measurement efficiency and time.
 - [17] W. Dür and H.-J. Briegel, *Phys. Rev. Lett.* **90**, 067901 (2003).
 - [18] H. J. Krenner *et al.*, *Phys. Rev. Lett.* **94**, 057402 (2005).
 - [19] On-chip cavities may also connect local nodes; see, for example, A. Wallraff *et al.*, *Nature (London)* **431**, 162 (2004).